Clinica Chimica Acta 488 (2019) 104–110

Contents lists available at ScienceDirect

Clinica Chimica Acta

journal homepage: www.elsevier.com/locate/cca

Next generation sequencing in family with MNGIE syndrome associated to optic atrophy: Novel homozygous POLG mutation in the C-terminal subdomain leading to mtDNA depletion

Rahma Felhi[a,*], Lamia Sfaihi[c,1], Majida Charif[b,1], Valerie Desquiret-Dumas[b,e], Céline Bris[b,e], David Goudenège[b,e], Leila Ammar-Keskes[d], Mongia Hachicha[c], Dominique Bonneau[b,e], Vincent Procaccio[b,e], Pascal Reynier[b,e], Patrizia Amati-Bonneau[b,e], Guy Lenaers[b], Faiza Fakhfakh[a,*]

[a] Molecular and Functional Genetics Laboratory, Faculty of Science of Sfax, University of Sfax, Tunisia
[b] MitoLab Team, Institut MitoVasc, UMR CNRS 6015, INSERM U1083, Angers University, Angers, France
[c] Department of Pediatry, University Hospital Hedi Chaker, Sfax, Tunisia
[d] Human Molecular Genetics Laboratory, Faculty of Medecine of Sfax, University of Sfax, Tunisia
[e] Department of Biochemistry and Genetics, University Hospital Angers, Angers, France

ARTICLE INFO

Keywords:
MNGIE
POLG
OPA1
mtDNA depletion
Pathogenic variants

ABSTRACT

Introduction: Mitochondrial diseases are a group of disorders caused mainly by the impairment of the mitochondrial oxidative phosphorylation process, due to mutations either in the mitochondrial or nuclear genome. Among them, the mitochondrial neuro-gastrointestinal encephalo-myopathy (MNGIE) syndrome affects adolescents or young adults, and is mostly caused by *TYMP* mutations encoding a cytosolic thymidine phosphorylase (TP).

Patients and methods: The present study reports the molecular investigation by next-generation re-sequencing of 281 nuclear genes, encoding mitochondrial proteins, of consanguineous family including two individuals with MNGIE syndrome associated to optic atrophy. Bioinformatic analysis was also performed in addition to mtDNA deletion screening and mtDNA copy number quantification in blood of the two patients which were carried out by solf clipping program and qPCR respectively.

Results: Next-generation re-sequencing revealed a novel homozygous c.2391G > T *POLG* mutation (p.M797I) co-occurring with the hypomorphic c.1311A > G *OPA1* variant (p.I437M). Analysis of the mitochondrial genome in the two patients disclosed mtDNA depletion in blood, but no deletion. Bio-informatics investigations supported the pathogenicity of the novel POLG mutation that is located in the C-terminal subdomain and might change POLG 3D structure, stability and function.

Conclusion: The novel homozygous p.M797I *POLG* mutation is responsible for MNGIE combined to optic atrophy and mtDNA depletion in the two patients.

1. Introduction

Mitochondrial diseases are a clinically heterogeneous group of inherited metabolic disorders, mainly characterized by the dysfunction of the mitochondrial respiratory chain affecting the oxidative phosphorylation [1]. They can be caused by mutations in either mitochondrial or nuclear genes, encoding structural proteins of the respiratory chain complexes, proteins involved in mitochondrial biogenesis and structure, or in the maintenance of the mitochondrial genome [2]. Clinical features characterizing mitochondrial diseases are usually extremely heterogeneous, affecting variable tissues with different degrees of severity [3]. The clinical and genetic heterogeneities of mitochondrial disorders render genotype-phenotype correlations difficult. In this respect, the mitochondrial neuro-gastrointestinal encephalo-myopathy (MNGIE) syndrome represents a fairly well defined syndrome, encountered in adolescence or young adulthood, characterized by severe

* Corresponding authors at: Molecular and Functional Genetics Laboratory, Faculty of Science of Sfax, University of Sfax, Route Soukra. Km 3, Sfax, Tunisia.
E-mail addresses: Rahma.90felhi@gmail.com (R. Felhi), Faiza.fakhfakh02@gmail.com (F. Fakhfakh).
[1] Equal contributors.

https://doi.org/10.1016/j.cca.2018.11.003
Received 1 October 2018; Accepted 2 November 2018
Available online 03 November 2018
0009-8981/

gastro-intestinal dysmotility, intestinal pseudo-obstruction, cachexia, progressive external ophthalmoplegia, peripheral neuropathy, and lactic acidosis [4,5]. This syndrome when associated with the hallmark feature of leukoencephalopathy, is caused by mutations in the nuclear TYMP gene encoding thymidine phosphorylase (TP) [6]. TP is an enzyme that catalyzes the phosphorylation of the thymidine and the deoxyuridine bases [7]. Mutations in *TP* gene cause loss of the enzyme activity, accumulation of the dUrd and dThd substrates in plasma and tissues, and secondary mtDNA instability, such as depletion, deletions and point mutations [8]. A MNGIE-like syndrome without leukoencephalopathy has been also reported associated with mutations in the *POLG* gene (MIM *174763) [9], encoding the polymerase gamma involved in the replication of the mtDNA. In addition, a MNGIE-like phenotype has been reported in a patient with recessive mutations in *RRM2B* [10], which encode the RIR2B protein (p53R2). *RRM2B* is transcriptionally regulated by the tumor suppressor TP53 and plays a key role in the stress response to various cell-damaging stimuli [11]. Mutations in *RRM2B* have also been reported to cause mtDNA depletion in patients presenting with early-onset seizures, hypotonia, diarrhea, renal tubulopathy and lactic acidosis [12].

In the present study, we report a consanguineous family with two boys presenting a severe MNGIE syndrome associated with optic atrophy. We performed next generation re-sequencing (NGS) using a custom-made targeted mitochondrial panel of 286 genes. Results revealed in the two patients a known heterozygous *OPA1* variation c.1311A > G (p.I437M) and a novel homozygous mutation c.2391G > T (p.M797I) in *POLG* gene associated with a 60% reduction of the mtDNA copy number. *In silico* analyses supported the pathogenicity of this novel *POLG* mutation and showed its effects on POLG stability, structure and activity.

2. Patients and methods

This study was carried out on a Tunisian family with four children, among them two individuals had clinical and biochemical symptoms suggestive of a MNGIE syndrome. Written informed consent was obtained from each subject involved in this study or from the parents of the subjects under 18 years of age, in agreement with the Declaration of Helsinki.

3. Clinical description

3.1. Patient 1

He is a 14-year-old boy, born at 40 weeks of gestation following an uncomplicated pregnancy. His psychomotor development was normal. At the age of 2, he developed a clumsy approach and frequent falls. The neurological signs worsened with age and he lost the ability to walk at the age of 8 years. Nerve conduction studies revealed bilateral sensorimotor neuropathy, particularly in the lower limbs. Brain magnetic resonance imaging (MRI) at age 11 was normal (Fig. 1A). At the age of 14, he was hospitalized for chronic weight loss, vomiting, abdominal pain and diarrhea for the past three years. The patient was cachectic (weight: 21 kg, height: 139 cm and body mass index: 10.9 kg/m^2). Clinical examination revealed generalized oedema, severe muscular atrophy, generalized muscle weakness and wastage mainly in the lower limbs, sensory neuropathy of the extremities and absence of tendon reflexes. His cognitive functions were normal. Cranial nerve functions were normal, but he had a slight left ptosis and a limitation of extraocular muscle function in adduction and elevation. Biological tests showed intestinal abnormal absorption and enteropathy with loss of protein and high level of lactate in the blood (4.98 mmol/l). Superior gastrointestinal endoscopy revealed no specific finding, and the pathological examination of the duodenal biopsy specimen was not compatible with gluten sensitive enteropathy (GSE). In addition, antibodies specific for GSE were negative in the patient's serum. Ophthalmological examination showed a decrease in visual acuity (6/10 in the left eye and 8/10 in the right) due to optic atrophy. Electroretinogram (ERG) was normal, whereas visual evoked potentials were impaired. The audiogram and auditory evoked potentials were normal. He died at the age of 15.

3.2. Patient 2

He is an 8-year-old boy born to term following an uncomplicated pregnancy. His developmental stages were largely delayed: control of the head was acquired at the age of 6 months; he sat without support at the age of 12 months and stood up with support at 24 months, but never walked. His cognitive development was normal. At the age of 8, he was cachectic; his weight was 20 kg, his height was 118 cm and his body mass index was 14.4 kg/m^2. Motor examination revealed widespread muscle weakness and wastage, especially in the lower limbs. All tendon reflexes were absent. The functions of the cranial nerve were normal. He had neither ptosis nor ophthalmoparesis. Fundus examination revealed bilateral optic atrophy and visual evoked potentials were altered. Nerve conduction studies revealed bilateral sensorimotor neuropathy, particularly in the lower limbs. Biochemical tests revealed an elevation of lactate in the blood (4.6 mmol/l), serum pyruvate: 0.18 mmol/l and a high lactate/pyruvate ratio: 25.5. The T2-weighted brain MRI showed a slight increase in signal, affecting the periventricular white matter of both hemispheres (Fig. 1B).

4. Methods

4.1. DNA extraction

Total DNA was extracted from peripheral blood using phenol chloroform standard procedures [13].

4.2. Molecular analysis

4.2.1. Library preparation and sequencing

A NGS panel of 281 nuclear genes encoding mitochondrial proteins involved in the most frequent mitochondrial pathologies was used to screen for mutations in the two patients. Library preparation for each sample was carried out using SureSelect Target Enrichment System for Sequencing on Ion Proton (Manuel number G7530-90005).

The entire mtDNA molecule was amplified with two over-lapping 8.5 kilo base (kb) fragments. Library preparation was performed using the Ion Plus Fragment Library Kit (Cat. no. 4471269).

Sample emulsion PCR, emulsion breaking, and enrichment were performed using the Ion PI™ Chip Kit v2 BC (Cat. no. 4484270) and Ion PI™ IC 200 Kit (Cat. no. 4488377) and sequencing was undertaken using sequencing with the Ion Proton™ System.

All sequencing data were processed using a dedicated bioinformatic pipeline, which includes the three variant analysis steps: calling, annotation and prioritization. The calling module uses a consensus-based approach and combines the prediction of 6 callers (VariantCaller include with the Torrent Suite, GATK Unified Genotyper [14], VarScan2 [15], SNVer [16], LoFreq [17] and Platypus [18]). All the generated VCFs (Variant Calling Format) are normalized and decomposed before launching the annotation-priorization module, which combines NCBI Variant Reporter and ANNOVAR [19]. These tools allow to include genomic databases like dbSNP, 1000G and ExAC v0.3 [20]), clinical databases like CLINVAR [21] and precomputed results of several priorization tools (e.g SIFT, PolyPhen2, LRT, MutationTaster).

4.2.2. Verification of variants by Sanger sequencing

All variants identified have been verified by Sanger sequencing. After PCR amplification, each PCR product was purified and subsequently analyzed by direct sequencing on an ABI PRISM 3100- Avant automated DNA sequencer using the BigDye Terminator Cycle

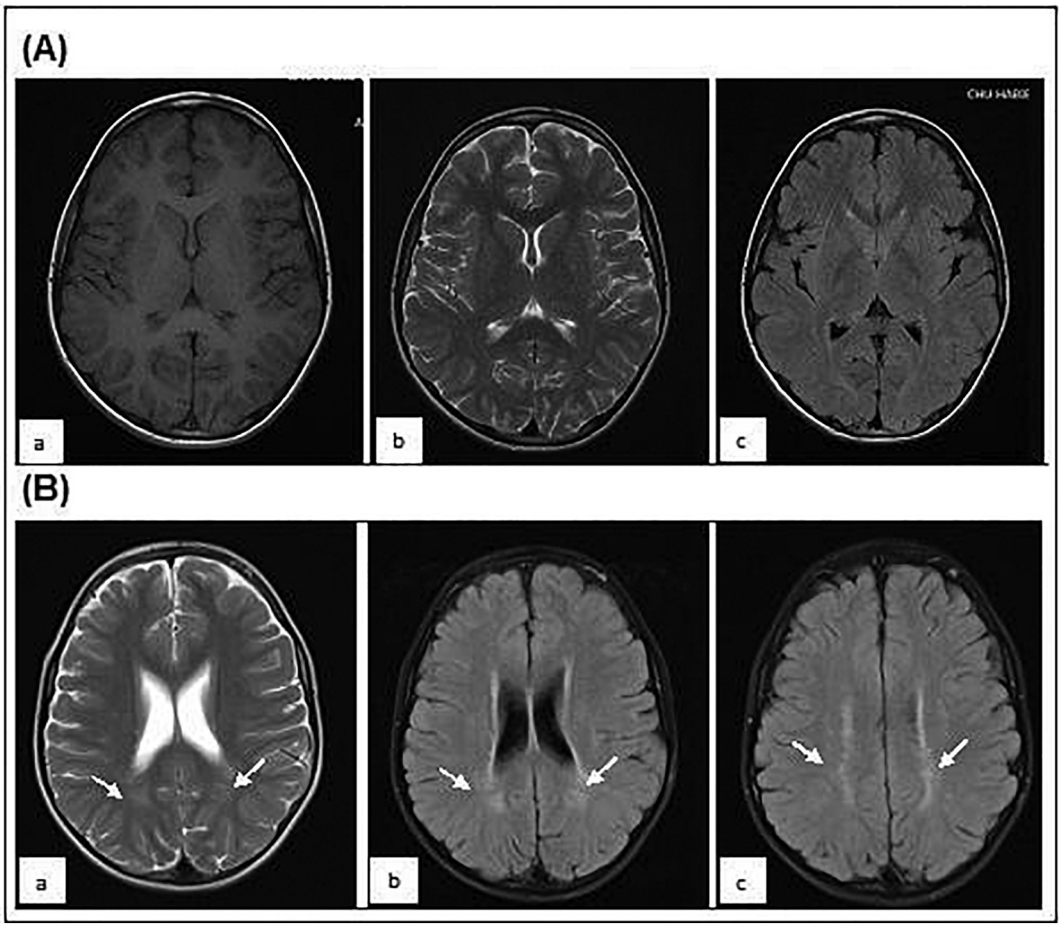

Fig. 1. (A) Brain MRI performed in patient 1 at the age of 11 years, showing a normal profile a) axial T1 weighted image, b) axial T2 weighted, c) axial FLAIR. (B) Brain MRI performed in patient 2 at the age of 8 years: a) axial T2-weighted image shows abnormal high signal intensity in the bilateral periventricular white matter (white arrows), b) and c): axial FLAIR showing the abnormal high signal intensity in the bilateral periventricular white matter (white arrows).

Sequencing reaction kit v1.1. Sequences were compared with the update Cambridge sequence (GenBank accession number: NC_012920).

4.2.3. Quantification of mtDMA copy number

The mtDNA copy number in blood was determined by real time quantitative polymerase chain reaction (qPCR) with primers specific for the mitochondrial and the nuclear genes, according to published protocols [22,23]. The primer sequences used for mitochondrial NADH dehydrogenase subunit 4 (*ND4*) and cytochrome *c* oxydase (*COXI*) genes and for the nuclear B-actin (*B2M*) and *GAPDH* genes are shown in Table 1. The qPCR was performed on a thermal cycler (Applied Biosystems StepOne™) by using the Syber Green chemistry (Applied Biosystems) including the following settings: 10 min at 95 °C, then 40 cycles of 30 s at 95 °C, 30 s at 52 °C and 15 s at 72 °C. The mtDNA copy number was determined according to the comparative method ΔΔCt, using the formula: $2 \times 2^{\Delta\Delta Ct}$ [24] and normalized to age matched controls (5 to 15 years old).

Table 1
Sequence of the primers used for real-time PCR quantification of the mtDNA.

Gene targeted	Sequence	Amplicon Size (pb)
ND4	F: 5′CGCACTAATTTACACTCA3′ R: 5′GCTAGTCATATTAAGTTGTTG3′	108
COX I	F: 5′TCCACTATGTCCTATCAATA3′ R: 5′GGTGTAGCCTGAGAATAG3′	83
B2M	F: 5′CAGCTCTAACATGATAACC3′ R: 5′CCTGTAGGATTCTTCTTTC3′	80
GAPDH	F: 5′CCCTGTCCAGTTAATTTC3′ R: 5′CACCCTTTAGGGAGAAAA3′	85

4.2.4. Long-range PCR amplification

A 16 kb fragment was amplified by PCR reaction using the Long PCR Enzyme Mix (# K0182) (Fermentas) and the following primers: 5' GGCACCCCTCTGACATCC 3′ and 5' TAGGTTTGAGGGGGAATGCT 3′ in a thermal cycler (Gen- Amp PCR System 9700; Applied Biosystem). The conditions for the PCR reaction were: initial denaturation at 94 °C for 1 min, followed by 32 cycles: 10 s at 98 °C, and 15 min at 68 °C and a final extension at 72 °C for 10 min. PCR Products were separated on 0.8% agarose gel, and visualized with ethidium bromide.

4.2.5. Bioinformatic tools

4.2.5.1. Sequence alignment and pathogenicity prediction. The evolutionary conservation of p.M797I was estimated using the Clustal Omega software, by alignment of the POLG protein sequence of different species obtained from the NCBI database (http://www.ebi.ac.uk/Tools/msa/clustalo/). The degree of pathogenicity of the *POLG* mutation was predicted using four *in silico* programs based on different approaches: Provean (http://provean.jcvi.org/seq_submit.php) bases its predictions on sequence conservation [25]; PolyPhen2 (http://genetics.bwh.harvard.edu/pph2/index.shtml) predicts possible impact of an amino acid substitution on the structure and function of a human protein, using physical and comparative considerations [26]. MutPred (http://mutpred.mutdb.org/index.html) estimates the impact of an amino-acid substitution, using a large panel of attributes related to protein structure and dynamics, the predicted functional properties,

and the amino acid sequence and evolutionary information [27]. A probability > 50% is considered as pathogenic. Mutation taster program (http://www.mutationtaster.org/) provides a testing criterion, called the "mutation adequacy score" [28].

The structural effects were predicted using the SNPeffect 4.0 database. Predictions included four properties of the protein to note aggregation tendency (TANGO), amyloid propensity (WALTZ), chaperone binding (LIMBO) and protein stability (FoldX). For each property, the difference of score between normal and mutated structure was calculated to evaluate the alteration [29].

4.2.5.2. Prediction of POLG 3D protein structure. The POLG 3D protein structure was performed using the RaptorX web server as a resource for template-based tertiary structure modeling [30]. The SWISS PDB VIEWER software (V4.1) was used to display and compare normal and mutated models [31]. The superposition of the two models ensures the calculation of the RMSD deviation, which measures the average distance between the backbone atoms of wild-type and mutated alleles. A high RMSD deviation indicates that the structural rearrangements caused by the substitution are important [32].

5. Results

5.1. Mutational analysis

In this report, we studied a consanguineous Tunisian family including two individuals with clinical features suggestive of MNGIE syndrome associated to optic atrophy. Next-Generation Sequencing of all exons of 281 nuclear genes encoding mitochondrial proteins was performed in the two patients. Variant filtering led to the identification of a novel homozygous substitution c.2391G > T (p.M797I) in exon 14 of *POLG* and the known c.1311A > G substitution (p.I437M) in *OPA1*, both were confirmed by Sanger sequencing (Fig. 2A).

The novel c.2391G > T mutation in *POLG* gene was present at homozygous state in the two affected individuals (P1 and P2), was heterozygous in the parents, and was absent in the unaffected sisters (Fig. 2B), as well as in 100 healthy controls from the Tunisian population. In addition, the two affected brothers were also heterozygous for the c.1311A > G *OPA1* (NM_130837.2) substitution, inherited from their father, while the mother and sisters were negative for this variant (Fig. 2B).

The novel c.2391G > T mutation in exon 14 of *POLG* substitutes the highly conserved methionine to isoleucine (p.M797I) at the C-terminal thumb subdomain of the POLG protein, (Fig. 3A). The multiple alignment of POLG protein sequences from different species showed that the thumb domain, including the p.M797 amino acid, is highly conserved across vertebrates (Fig. 3B).

The pathogenicity of p.M797I was predicted *in vitro* by several bioinformatics softwares. Polyphen-2 predicted that p.M797I is possibly damaging, while Provean, MutPred and Mutation Taster programs classified it as "deleterious" and 'disease causing'.

We analyzed the 3D models of both wild-type and mutant POLG protein using the Deep View/Suiss-PDB viewer4.1 program. The root mean square deviation (RMSD) for backbone atoms between the two structures was significant (RMSD = 11.43 Å), suggesting that the overall architecture of the mutant protein is very different from that of the wild-type POLG protein (Fig. 3C). In addition, the comparison of normal and mutated 3D models showed that the p.M797I mutation adds new hydrogen bound between N795 and C796 in the mutated protein that may affect POLG spatial conformation (Fig. 3C; a-b).

Moreover, the superposition of both wild type and mutated models in the region covering specifically the thumb subdomain encompassing amino acids 785–815 showed conformational changes (Fig. 3C; c-d).

Predictive results displayed by the SNPeffect 4.0 tool confirmed the structural defect. In fact, based on FoldX, it has been shown that the mutation from Methionine to Isoleucine at position 797 results in a ddG of 0.89 kcal/mol. This implies that the mutation reduces the protein stability. Further, dLIMBO score equals −236.17 which means that the mutation decreased the chaperone binding tendency of the POLG polymerase. Together, these analyzes converge to a damaging effect of this mutation on the structure, stability and activity of the mutated POLG protein.

5.2. MtDNA analysis

Next Generation Sequencing of the whole mitochondrial genome revealed the presence of several reported variations, but none of them was pathogenic. Furthermore the q-PCR analysis showed a 60% decrease of mtDNA content compared to the average of healthy control values from individuals aged between 5 and 15 years (Table 2). Furthermore, the value of mtDNA copy number in the blood from the patients' mother was normal. In addition, we performed a Long Range PCR of a 16 kb mtDNA fragment in both patients and a healthy individual. Results revealed the absence of mitochondrial deletion in the

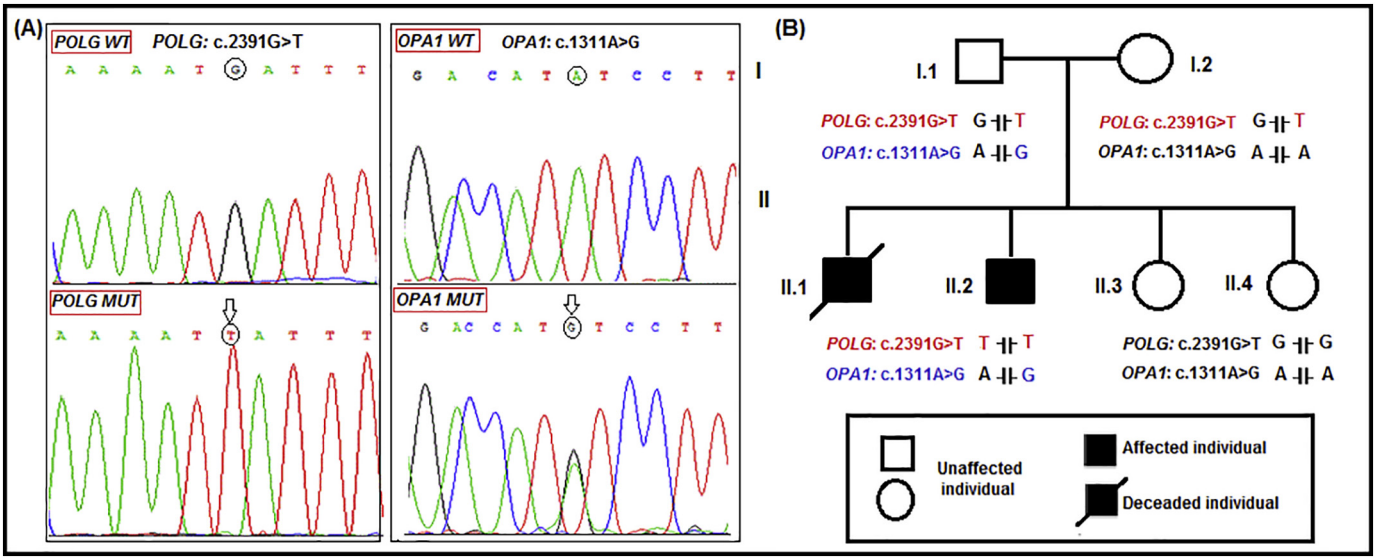

Fig. 2. (A) Sequencing chromatogram showing the novel homozygous c.2391G > T variation in *POLG* and the heterozygous c.1311 A > G variation in *OPA1* in affected individuals compared to their unaffected sister. (B) Pedigree of the studied family presenting the segregation of *POLG* and *OPA1* mutations.

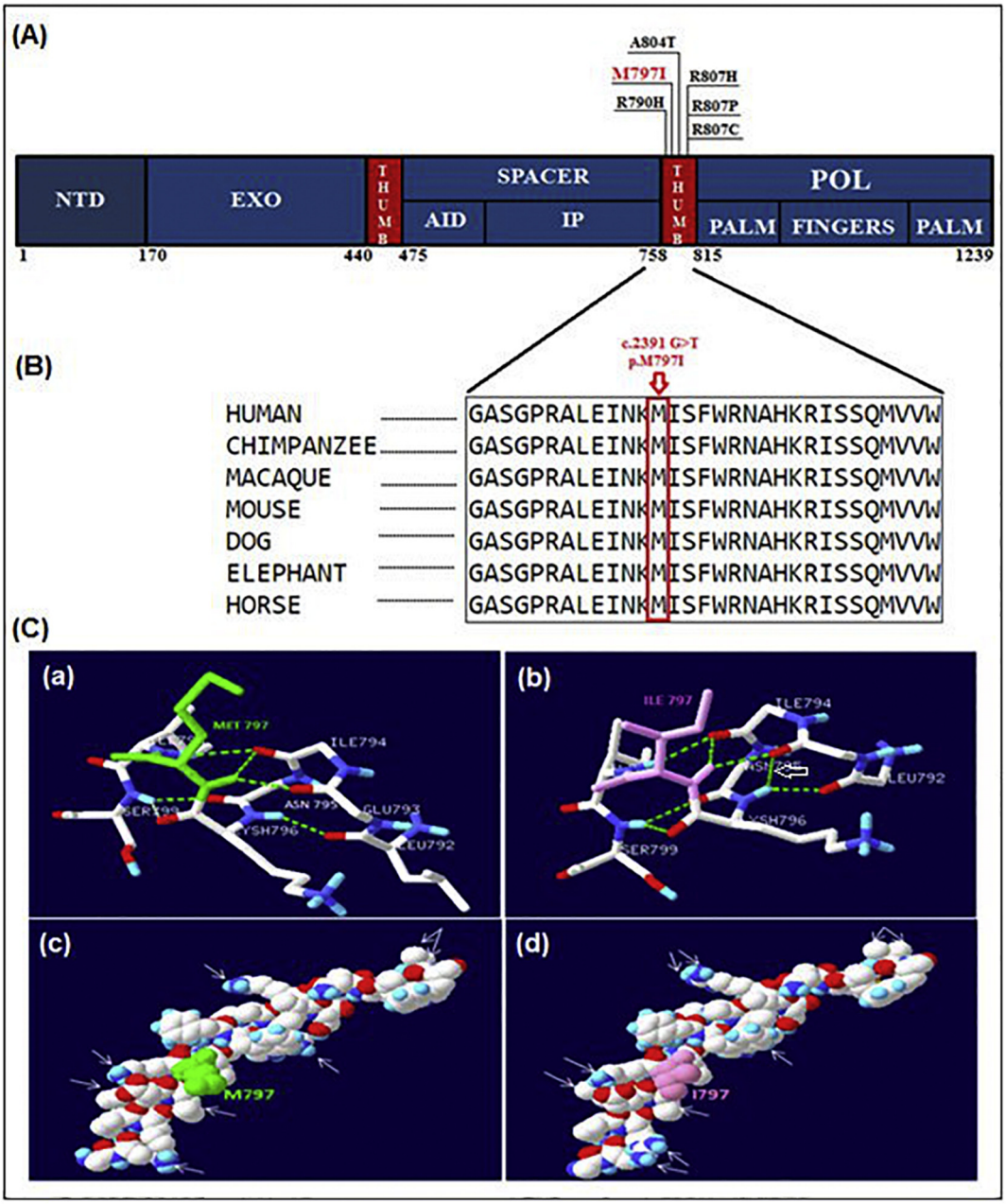

Fig. 3. (A) Schematic representation of the novel and previous variations in the C-terminal Thumb region of the POLG protein. (B) Global alignment of the amino acid sequence of the Thumb subdomain (amino acids 785–815) in POLG protein from 7 different vertebrate species. (C) Molecular modeling of POLG protein. The 3D structure modelization shows the hydrogen bounds between the mutated and wild type amino acids with other residues (a-b) and the addition of hydrogen bound between the residues 795 and 796 (c–d). The overall architecture of both normal and mutated proteins at the C-terminal thumb subdomain shows a change in the conformation of the p.I797 mutated protein (c) compared to the normal one (d).

Table 2
Calculation of the mtDNA copy number in the patients, the mother and control individuals.

Individual	ΔΔCt ΔCt (mean NUC) − ΔCt (mean MITO)	mtDNA copy number ($2 \times 2^{\Delta\Delta Ct}$)	RQ (%)
P1	6.03	130.68	40.05
P2	6.14	141.04	43.22
Mother	7.05	265.2	81.27
Controls (n = 20)	7.35	326.28[a]	100

[a] Standard Deviation = 40.04, RQ: Relative Quantification.

explored fragment in affected and control individuals.

6. Discussion

Here, we performed Next Generation Sequencing (NGS) on DNA from two affected brothers from a consanguineous family with clinical features of MNGIE syndrome associated to optic atrophy. The screening of 281 nuclear genes encoding mitochondrial proteins revealed a novel homozygous mutation c.2391G > T (p.M797I) in *POLG* and the known variation c.1311A > G (p.I437M) in *OPA1*. In addition, the mtDNA copy number of both patients disclosed a 60% decrease in blood.

The POLG methionine residue at position 797 is well conserved across species located in the highly conserved C-terminal thumb

Table 3
Summary of the *in silico* analysis and the molecular modeling of pathogenic variations reported in the C-terminal thumb subdomain.

Variation	Polyphen	Provean	Mutpred	Mutation taster	RMSD	Reference
R790H	Probably damaging	Deleterious	60.9%	Disease causing	4.90 Å	Tang et al. [37]
M797I	**Possibly damaging**	**Deleterious**	**62.5%**	**Disease causing**	**11.43 Å**	**This study**
A804T	likely benign	Neutral	88.4%	Disease causing	3.25 Å	Blok et al. [42]
R807P	Probably damaging	Deleterious	95.9%	Disease causing	11.12 Å	Del Bo et al. [38]
R807H	Probably damaging	Deleterious	90.9%	Disease causing	8.38 Å	Tang et al. [37]

RMSD: Root Mean Square Deviation.

Table 4
Homozygous and heterozygous composite *POLG* mutations located in the C-Terminal thumb subdomain with the associated clinical phenotypes.

Mutation amino acid change	Main syndrome	Optic atrophy	Genetics	Reference
2369 G > A R790H	Alpers syndrome	No	HT	Tang et al. [37]
2391 G > T M797I	**MNGIE syndrome**	**Yes**	**HM**	**This study**
2410 G > A A804T	Muscle complaints, and bulbar dysarthria	No	HT	Blok et al. [42]
2419 G > T R807C	Ptosis and myopathy	No	HT	Ferreira et al. [43]
	Encephalopathy, liver failure, and lactic acidosis	No	HT/A467T	Tang et al. [37]
2420 G > A R807H	Seizures and hepatic failure, hypotonia, and failure to thrive	No	HT/A467T	Tang et al. [37]
2420 G > C R807P	PEO	No	Sporadic, HT/T251I	Del Bo et al. [38]

HM: Homozygous, HT: Heterozygous.

subdomain. Several bioinformatics tools predicted that this mutation is highly damaging and deleterious.

In addition, SWISS PDB VIEWER software revealed that the p.M797I change leads to conformational changes of POLG global structure and in the C-terminal thumb subdomain, with a highly significant RMSD (11.43 Å), suggesting the importance of the methionine residue in this domain. Moreover, the decrease in the protein stability and in chaperone binding tendency of the mutated POLG could affect the flexibility, activity and the efficacity of this DNA polymerase.

To date, five other mutations (R790H, A804T, R807H, R807P and R807C) were described in POLG thumb domain (http://polg.bmb.msu.edu/). Given the limited studies of the structure of this domain, we predicted the structural effects of these mutations and compared them to the one induced by the M797I substitution. Results revealed that all the previously identified mutations have a high RMSD score (RMSD > 3), but lower than that of the p.M797I mutation (Table 3), thus further supporting the pathogenicity of the p.M797I amino acid change. This thumb domain is included in the partitioning loop of Cluster 3, which is part of five functional modules, called clusters 1 to 5, assigned to POLG structure [33].

Bioinformatic investigations performed here for the p.M797I mutation are also in agreement with functional studies previously carried out for some specific mutations in cluster 3, which indicated that they affected both the DNA binding affinity and the catalytic activity [34]. In addition, one study showed that yeast carrying Polγ mutations in residues from the thumb subdomain altered the polymerase and/or exonuclease activities [35]. From these data, we conclude that mutations in the C-terminal thumb domain are pathogenic and affect mitochondrial POLG structure and activity, affecting its replication efficiency [36]. This is in agreement with the fact that both patients exhibited a 60% mtDNA depletion in their blood sample.

Furthermore, mutations in *POLG* were associated with a large range of different clinical phenotypes, including Alpers syndrome [36,37], progressive external ophthalmoplegia (PEO) [38] and other severe adult disorders such as Parkinson and SANDO syndromes [39]. Since 2003, recessive mutations in *POLG* were described in patients with MNGIE syndrome [40], while before, this syndrome was only known to be associated to *TYMP* mutations [41]. Recently, *POLG* mutations were also described in MNGIE-Like syndromes [9]. Nevertheless, our report provides the first evidence of a mutation in POLG thumb domain associated with the MNGIE syndrome. Indeed, pathogenic variants in this domain have been associated with other phenotypes, such as muscle complaints and dysarthria with the p.A804T [42], Alpers syndrome with the p.R807H [38], PEO syndrome with the p.R807P [39] and SANDO and Alpers syndromes, respectively with the p.R807C and p.R807H mutations in compound heterozygous state associated with other mutations [37,44] (Table 4).

Furthermore, pathogenic mutations in POLG gene were very scarcely reported associated to optic atrophy [45], and virtually no POLG mutation in the C-Terminal thumb domain was associated with optic atrophy (Table 4). Here, the new p.M797I deleterious mutation found in this domain seems to be responsible for the optic atrophy and MNGIE manifested by the two patients although they also shared the heterozygous OPA1 p.I437M variation which was previously described associated with optic atrophy [46]. Indeed this variant was also present at heterozygous state in the unaffected father and in whom no optic atrophy was observed. The *OPA1* variant p.I437M has always been reported associated with another OPA1 variation such as in patients with syndromic autosomal dominant optic atrophy or with the Behr syndrome [46–48].

In conclusion, the NGS analysis of a consanguineous family with MNGIE syndrome plus optic atrophy revealed a novel homozygous *POLG* mutation c.2391G > T (p.M797I), co-occurring with the known *OPA1* variant p.I437M. Bioinformatic investigations supported the pathogenicity of the novel (p.M797I) mutation and classify it as damaging and deleterious. Furthermore and interestingly, this mutation was located in the POLG C-terminal subdomain, leading to a major change in protein 3D structure probably affecting POLG stability and function, ultimately leading to the mtDNA depletion in the two patients.

Conflict of interest statement

The authors declare no conflict of interest. The authors alone are responsible for the content and writing of the paper.

Author contributions

Felhi, Charif, Lenaers and Fakhfakh had full access to all of the data in the study and take responsibility for the integrity of the data and the accuracy of the data analysis. Analysis or interpretation of data: Felhi, Charif, Desquiret-Dumas, Bris, Goudenège, Ammar-Keskes, Bonneau, Procaccio, Reynier, Amati-Bonneau, Lenaers and Fakhfakh. Draft of the manuscript: Felhi, Charif, Sfaihi, Lenaers and Fakhfakh. Critical revision of the manuscript for important intellectual content: Bonneau, Procaccio, Reynier, Amati-Bonneau, Lenaers and Fakhfakh.

Acknowledgments

We would like to thank all the member of the family for their cooperation in the present study. This work was supported by the Ministry of Higher Education and Scientific Research in Tunisia, University of Sfax. We acknowledge the support from the Institut National de la Santé et de la Recherche Médicale (INSERM), France; Centre National de la Recherche Scientifique (CNRS), France; the Université d'Angers, the University Hospital of Angers, the Région Pays de Loire and Angers Loire Métropole, France.

References

[1] M.R. Chiaratti, F.V. Meirelles, D. Wells, J. Poulton, Therapeutic treatments of mtDNA diseases at the earliest stages of human development, Mitochondrion 11 (2011) 820–828.
[2] J.F. Montiel-Sosa, M.D. Herrero, M.D.L. Munoz, L.E. Aguirre-Campa, G. Pérez-Ramírez, R. García-Ramírez, et al., Phylogenetic analysis of mitochondrial DNA in a patient with Kearns–Sayre syndrome containing a novel 7629-bp deletion, Mitochondrial DNA 24 (2013) 420–431.
[3] G.S. Gorman, P.F. Chinnery, S. Dimaur, M. Hirano, Y. Koga, R. McFarland, et al., Mitochondrial diseases, Nat. Rev. Dis. Prim. 2 (2016) 16080.
[4] F. Demaria, F. De Crescenzo, A.M. Caramadre, A. D'Amico, A. Diamanti, F. Fattori, et al., Mitochondrial neurogastrointestinal encephalomyopathy presenting as anorexia nervosa, J. Adolesc. Health 59 (2016) 729–731.
[5] M. Hirano, Y. Nishigaki, R. Martí, Mitochondrial neurogastrointestinal encephalomyopathy (MNGIE): a disease of two genomes, Neurologist 10 (2004) 8–17.
[6] I. Nishino, A. Spinazzola, M. Hirano, Thymidine phosphorylase gene mutations in MNGIE, a human mitochondrial disorder, Science 283 (1999) 689–692.
[7] Z. Barış, T. Eminoğlu, B. Dalgıç, L. Tümer, A. Hasanoğlu, Mitochondrial neurogastrointestinal encephalomyopathy (MNGIE): case report with a new mutation, Eur. J. Pediatr. 169 (2010) 1375–1378.
[8] A.W. El-Hattab, F. Scaglia, Mitochondrial DNA depletion syndromes: review and updates of genetic basis, manifestations, and therapeutic options, Neurotherapeutics 10 (2013) 186–198.
[9] P. Prasun and D.D. Koeberl, Mitochondrial neurogastrointestinal encephalomyopathy (MNGIE)-like phenotype in a patient with a novel heterozygous POLG mutation J. Neurol., 261 (2014) 1818.
[10] A. Shaibani, O.A. Shchelochkov, S. Zhang, P. Katsonis, O. Lichtarge, L.J. Wong, et al., Mitochondrial neurogastrointestinal encephalopathy due to mutations in RRM2B, Arch. Neurol. 66 (2009) 1028–1032.
[11] H. Tanaka, H. Arakawa, T. Yamaguchi, K. Shiraishi, S. Fukuda, K. Matsui, et al., A ribonucleotide reductase gene involved in a p53-dependent cell-cycle checkpoint for DNA damage, Nature 404 (2000) 42.
[12] A. Bourdon, L. Minai, V. Serre, J.P. Jais, E. Sarzi, S. Aubert, et al., Mutation of RRM2B, encoding p53-controlled ribonucleotide reductase (p53R2), causes severe mitochondrial DNA depletion, Nat. Genet. 39 (2007) 776.
[13] H.A. Lewin, A simple method for DNA extraction from leukocytes for use in PC, Biotechniques 13 (1992) 522–524.
[14] A. McKenna, M. Hanna, E. Banks, A. Sivachenko, K. Cibulskis, A. Kernytsky, et al., The Genome Analysis Toolkit: a MapReduce framework for analyzing next-generation DNA sequencing data, Genome Res. 20 (2010) 1297–1303.
[15] D.C. Koboldt, K.M. Steinberg, D.E. Larson, R.K. Wilson, E.R. Mardis, The next-generation sequencing revolution and its impact on genomics, Cell 155 (2013) 27–38.
[16] Z. Wei, W. Wang, P. Hu, G.J. Lyon, H. Hakonarson, SNVer: a statistical tool for variant calling in analysis of pooled or individual next-generation sequencing data, Nucleic Acids Res. 39 (2011) e132.
[17] A. Wilm, A.W. Ppk, D. Bertrand, G.H.T. Yeo, S.H. Ong, C.H. Wong, et al., LoFreq: a sequence-quality aware, ultra-sensitive variant caller for uncovering cell-population heterogeneity from high-throughput sequencing datasets, Nucleic Acids Res. 40 (2012) 11189–11201.
[18] A. Rimmer, H. Phan, I. Mathieson, Z. Iqbal, S.R. Twigg, A.O. Wilkie, et al., Integrating mapping-, assembly-and haplotype-based approaches for calling variants in clinical sequencing applications, Nat. Genet. 46 (2014) 912.
[19] H. Yang, K. Wang, Genomic variant annotation and prioritization with ANNOVAR and wANNOVAR, Nat. Protoc. 10 (2015) 1556.
[20] E.M. Smigielski, K. Sirotkin, M. Ward, S.T. Sherry, dbSNP: a database of single nucleotide polymorphisms, Nucleic Acids Res. 28 (2000) 352–355.
[21] M.J. Landrum, J.M. Lee, G.R. Riley, W. Jang, W.S. Rubinstein, D.M. Church, D.R. Maglott, ClinVar: public archive of relationships among sequence variation and human phenotype, Nucleic Acids Res. 42 (2013) D980–D985.
[22] R.K. Bai, L.J.C. Wong, Simultaneous detection and quantification of mitochondrial DNA deletion (s), depletion, and over-replication in patients with mitochondrial disease, J. Mol. Diagn. 7 (2005) 613–622.
[23] D. Dimmock, L.Y. Tang, E.S. Schmitt, L.J.C. Wong, Quantitative evaluation of the mitochondrial DNA depletion syndrome, Clin. Chem. 56 (2010) 1119–1127.
[24] V. Venegas, J. Wang, D. Dimmock, L.J. Wong, Real-time quantitative PCR analysis of mitochondrial DNA content, Curr. Protoc. Hum. Genet. (2011) 19–27.
[25] Y. Choi, A.P. Chan, PROVEAN web server: a tool to predict the functional effect of amino acid substitutions and indels, Bioinformatics 31 (2015) 2745–2747.
[26] I. Adzhubei, D.M. Jordan, S.R. Sunyaev, Predicting functional effect of human missense mutations using PolyPhen-2, Curr. Protoc. Hum. Genet. (2013) 7–20.
[27] B. Li, V.G. Krishnan, M.E. Mort, F. Xin, K.K. Kamati, D.N. Cooper, et al., Automated inference of molecular mechanisms of disease from amino acid substitutions, Bioinformatics 25 (2009) 2744–2750.
[28] J.M. Schwarz, C. Rödelsperger, M. Schuelke, D. Seelow, MutationTaster evaluates disease-causing potential of sequence alterations, Nat. Methods 7 (2010) 575.
[29] G. De Baets, J. Van Durme, J. Reumers, S. Maurer-Stroh, P. Vanhee, J. Dopazo, et al., SNPeffect4.0: on-line prediction of molecular and structural effects of proteincoding variants, Nucleic Acids Res. 40 (2012) 935–939.
[30] M. Källberg, G. Margaryan, S. Wang, J. Ma, J. Xu, RaptorX server: a resource for template-based protein structure modeling, Protein Structure Prediction, Humana Press, 2014, pp. 17–27.
[31] N. Guex, M.C. Peitsch, SWISS-MODEL and the Swiss-Pdb Viewer: an environment for comparative protein modeling, Electrophoresis 18 (1997) 2714–2723.
[32] O. Carugo, S. Pongor, A normalized root-mean-spuare distance for comparing protein three-dimensional structures, Protein Sci. 10 (2001) 1470–1473.
[33] A. Nurminen, G.A. Farnum, L.S. Kaguni, Pathogenicity in POLG syndromes: DNA polymerase gamma pathogenicity prediction server and database, BBA Clin. 7 (2017) 147–156.
[34] L. Euro, E. Farnum, A. Palin, L.S. Suomalainen, Kaguni, Clustering of Alpers disease mutations and catalytic defects in biochemical variants reveal new features of molecular mechanism of the human mitochondrial replicase, Pol γ, Nucleic Acids Res. 39 (2011) 9072–9084.
[35] F. Foury, K. Szczepanowska, Antimutator alleles of yeast DNA polymerase gamma modulate the balance between DNA synthesis and excision, PLoS One 6 (2011) e27847.
[36] R. Kasiviswanathan, W.C. Copeland, Biochemical analysis of the G517V POLG variant reveals wild-type like activity, Mitochondrion 11 (2011) 929–934.
[37] S. Tang, J. Wang, N.C. Lee, M. Milone, M.C. Halberg, E.S. Schmitt, et al., Mitochondrial DNA polymerase γ mutations: an ever expanding molecular and clinical spectrum, J. Med. Genet. 48 (2011) 669–681.
[38] R. Del Bo, A. Bordoni, M. Sciacco, A. Di Fonzo, S. Galbiati, M. Crimi, et al., Remarkable infidelity of polymerase γA associated with mutations in POLG1 exonuclease domain, Neurology 61 (2003) 903–908.
[39] R. Miguel, M.F. Gago, J. Martins, P. Barros, J. Vale, M.J. Rosas, POLG1-related levodopa-responsive Parkinsonism, Clin. Neurol. Neurosurg. 126 (2014) 47–54.
[40] G. Van Goethem, M. Schwartz, A. Löfgren, B. Dermaut, C. Van Broeckhoven, J. Vissing, Novel POLG mutations in progressive external ophthalmoplegia mimicking mitochondrial neurogastrointestinal encephalomyopathy, Eur. J. Hum. Genet. 11 (2003) 547.
[41] I. Nishino, A. Spinazzola, M. Hirano, MNGIE: from nuclear DNA to mitochondrial DNA, Neuromuscul. Disord. 11 (2001) 7–10.
[42] M.J. Blok, B.J. Van den Bosch, E. Jongen, A. Hendrickx, C.E. de Die-Smulders, J.E. Hoogendijk, et al., The unfolding clinical spectrum of POLG mutations, J. Med. Genet. 46 (2009) 776–785.
[43] M. Ferreira, T. Evangelista, L.S. Almeida, J. Martins, M.C. Macario, E. Martins, et al., Relative frequency of known causes of multiple mtDNA deletions: two novel POLG mutations, Neuromuscul. Disord. 21 (2011) 483–488.
[44] M.F. Gago, M.J. Rosas, J. Guimarães, M. Ferreira, L. Vilarinho, L. Castro, S. Carpenter, SANDO: two novel mutations in POLG1 gene, Neuromuscul. Disord. 16 (2006) 507–509.
[45] M. Milone, J. Wang, T. Liewluck, L.C. Chen, J.A. Leavitt, L.J. Wong, Novel POLG splice site mutation and optic atrophy, Arch. Neurol. 68 (2011) 806–811.
[46] S. Schimpf, N. Fuhrmann, S. Schaich, B. Wissinger, Comprehensive cDNA study and quantitative transcript analysis of mutant OPA1 transcripts containing premature termination codons, Hum. Mutat. 29 (2008) 106–112.
[47] T. Bonifert, K.N. Karle, F. Tonagel, M. Batra, C. Wilhelm, Y. Theure, et al., Pure and syndromic optic atrophy explained by deep intronic OPA1 mutations and an intralocus modifier, Brain 137 (2014) 2164–2177.
[48] D. Bonneau, E. Colin, F. Oca, M. Ferré, A. Chevrollier, N. Guéguen, et al., Early-onset Behr syndrome due to compound heterozygous mutations in OPA1, Brain 137 (2014) e301.